

# Neural Bipartite Matching

Dobrik Georgiev<sup>1</sup> Pietro Lió<sup>1</sup>

## Abstract

Graph neural networks have found application for learning in the space of algorithms. However, the algorithms chosen by existing research (sorting, Breadth-First search, shortest path finding, etc.) are usually trivial, from the viewpoint of a theoretical computer scientist. This report describes how neural execution is applied to a *complex* algorithm, such as finding maximum bipartite matching by reducing it to a flow problem and using Ford-Fulkerson to find the maximum flow. This is achieved via neural execution based only on features generated from a single GNN. The evaluation shows strongly generalising results with the network achieving *optimal matching* almost 100% of the time.

## 1. Introduction

Many real-world problems can be formulated as graph problems – social relations, protein folding, web search, etc. Throughout the years graph algorithms for solving these tasks have been discovered. One such task is the problem of finding the maximum flow  $f$  from a source to a sink in a graph  $G(V, E)$  whose edges have certain capacities  $c(u, v)$ ,  $(u, v) \in E$ . (Imagine material flowing source  $\rightsquigarrow$  sink). Any flow must obey two important properties: the flow on each edge should not exceed the capacity, i.e.  $f(u, v) < c(u, v)$  and for all nodes except source and sink flow should be preserved, i.e.  $\sum_{v \in V} f(u, v) = \sum_{v \in V} f(v, u)$ . Algorithms for finding maximum flow have found applications in many areas, such as bipartite matching (attempted here), airline scheduling or image segmentation (Boykov & Funka-Lea, 2006).

The main topic of this work is evaluating whether graph neural networks (GNNs) are able to reason like a *complex*

<sup>1</sup> Department of Computer Science and Technology, University of Cambridge, Cambridge, United Kingdom . Correspondence to: Pietro Lió <pietro.lió@cst.cam.ac.uk>, Dobrik Georgiev <dgg30@cam.ac.uk>.

*Proceedings of the 37<sup>th</sup> International Conference on Machine Learning*, Vienna, Austria, PMLR 108, 2020. Copyright 2020 by the author(s).

algorithm, specifically, whether they can be used for finding optimal bipartite matching using the Ford-Fulkerson (Ford & Fulkerson, 1956) algorithm for finding maximum flow. Performing the reasoning is achieved via neural execution, in a similar fashion to Veličković et al. (2020). GNNs have been both empirically (Veličković et al., 2020) and theoretically (Xu et al., 2020) shown to be applicable to algorithmic tasks on graphs, *strongly generalising* on inputs of sizes much larger than trained on. However, the algorithms tackled (BFS, Bellman-Ford (Bellman, 1958), etc.) have been relatively simple, consisting of a single subroutine performing a single operation until termination.

Our contributions are three-fold: **1)** We successfully show that GNNs are suitable for learning a complex algorithm, namely Ford-Fulkerson, which consists of several *composable* subroutines. To the best of our knowledge, this is the first time such an algorithm is neurally executed with GNNs. **2)** We demonstrate that GNNs can learn to respect the invariants of a complex algorithm. **3)** We devised an evaluation which not only separately takes into account the accuracy of the subroutines, but assesses the performance of the Ford-Fulkerson algorithm *as a whole* – an inconsistency even in one of the subroutines can invalidate the whole algorithm.

## 2. Background

### 2.1. Ford-Fulkerson

For presentational purposes consider a concise version of Ford-Fulkerson algorithm given in Cormen et al. (2009) which operates directly on the residual graph  $G_f$  with residual capacities  $c_f$  derived from the input flow graph. The source and sink of the network are *src* and *sink*:

#### Algorithm 1 Ford-Fulkerson

```

Input:  $G_f, \text{src}, \text{sink}$ 
while  $\exists$  valid path  $p \in G_f$  from src to sink do
     $c_f(p) = \min\{c_f(u, v) : (u, v) \in p\}$ 
    for each  $(u, v) \in p$  do
         $c_f(u, v) = c_f(u, v) - c_f(p)$ 
         $c_f(v, u) = c_f(v, u) + c_f(p)$ 
    end for
end while
return  $\sum_{v \in G} c_f(v, \text{src})$ 

```

The algorithm above has three key subroutines the neural network has to learn – finding augmenting path, finding minimum (bottleneck) capacity on the path and augmenting the residual capacities along the path.

## 2.2. Algorithm Execution

**Preliminary definitions** The GNN receives a sequence of  $T \in \mathbb{N}$  graphs with the same structure (vertices edges), but different features representing the execution of an algorithm. Let the graph be  $G(V, E)$ . At each timestep  $t \in \{1, \dots, T\}$ , each node  $i \in V$  has *node features*  $\vec{x}_i^{(t)} \in \mathbb{R}^{N_x}$  and each edge  $(i, j) \in E$  has *edge features*  $\vec{e}_{ij}^{(t)} \in \mathbb{R}^{N_e}$ . At each step of the algorithm node-level outputs  $\vec{y}_i^{(t)} \in \mathbb{R}^{N_y}$  are produced, which are later reused in  $\vec{x}_i^{(t+1)}$ .

**Encode-process-decode** The execution of an algorithm proceeds by the encode process decode paradigm (Hamrick et al., 2018). For each algorithm  $A$ , an *encoder network*  $f_A$  produces the algorithm-specific inputs  $\vec{z}_i^{(t)}$ . The result is then processed using the *processor network*  $P$ , which is shared across all algorithms. The processor takes as input encoded inputs  $\mathbf{Z}^{(t)} = \{\vec{z}_i^{(t)}\}_{i \in V}$  and edge features  $\mathbf{E}^{(t)} = \{\vec{e}_{ij}^{(t)}\}_{e \in E}$  to produce latent features  $\mathbf{H}^{(t)} = \{\vec{h}_i^{(t)}\}_{i \in V} \in \mathbb{R}^K$ . Algorithm specific outputs are calculated by its corresponding *decoder network*  $g_A$ . Termination of the algorithm is decided by a *termination network*,  $T_A$ , specific for each algorithm. The probability of the termination of an algorithm is obtained by applying the logistic sigmoid activation  $\sigma$  to the outputs of  $T_A$ . This is summarised as:

$$\vec{z}_i^{(t)} = f_A(\vec{x}_i^{(t)}, \vec{h}_i^{(t-1)}) \quad (1)$$

$$\mathbf{H}^{(t)} = P(\mathbf{Z}^{(t)}, \mathbf{E}^{(t)}) \quad (2)$$

$$\vec{y}_i^{(t)} = g_A(\vec{z}_i^{(t)}, \vec{h}_i^{(t)}) \quad (3)$$

$$\tau^{(t)} = \sigma(T_A(\mathbf{H}^{(t)})) \quad (4)$$

where  $\overline{\mathbf{H}^{(t)}} = \frac{1}{|V|} \sum_{i \in V} \vec{h}_i^{(t)}$ . The execution of the algorithm proceeds while  $\tau^{(t)} > 0.5$  and  $t < |V - 1|$ . The algorithm is *always* terminated in  $|V - 1|$  steps.

**Supervising algorithm execution** The aim for every algorithm is to learn to replicate the actual execution as close as possible. To achieve this, the supervision signal is driven by the actual algorithm outputs at every step  $t$ .

For more details, please refer to Veličković et al. (2020).

## 3. Neurally Executing Ford-Fulkerson

On a high-level, execution proceeds as in Figure 1. The neural network computes an augmenting path from an input

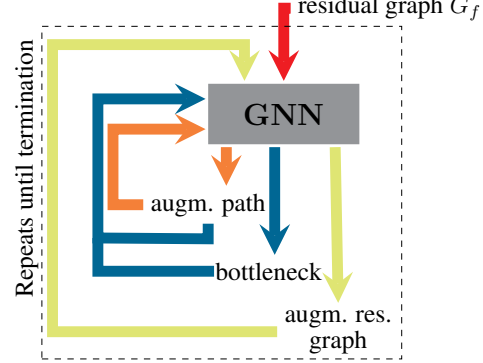
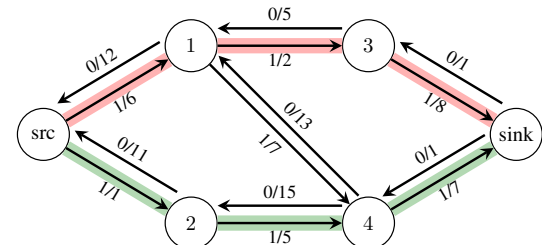


Figure 1. Neural execution of Ford-Fulkerson: The GNN takes as input a residual graph  $G_f$ . At each step of the algorithm, the GNN computes the augmenting path which is then reused (orange) to find the bottleneck edge on the path. The bottleneck and the augmenting path are then fed through (blue) to produce the residual graph with augmented capacities. The resulting residual graph is the input to the next step (yellow).

residual graph. Then, given the path, the bottleneck on it is found and the capacities on the path are changed according to Algorithm 1. The resulting new residual graph is reused as input to the next step and this process repeats until termination of the algorithm.

**Finding Augmenting Path** One of the key challenges to the task of finding an augmenting path was deciding how the supervision signal is generated. Supervising towards algorithms such as Breadth-First/Depth-First search turned out to be too difficult to train, since the algorithm and the learner could choose a different augmenting path (in both cases valid), but the learner is ‘penalised’ for its decision.



The solution to this problem is presented above. Additional weights are attached to each edge (edges are in the format *capacity/weight*). Now, if we choose to find the shortest path<sup>1</sup>, the bottom path (green) is preferred over the top one (red). This changes the task from finding an augmenting path to finding the *shortest* augmenting path, given the additional weights. Finding the shortest path with the Bellman-Ford algorithm (Bellman, 1958) can be achieved by learning to predict predecessors for each node (Veličković et al., 2020).

<sup>1</sup>It is theoretically possible that two shortest paths exist, but in practice this rarely occurred.

The network needs to learn to ignore zero capacity edges.

**Bottleneck Finding** After an augmenting path is found, the next step is to find the bottleneck capacity along this path. All edges not on the augmenting path are masked out (deterministically) and each edge is assigned a probability of being the bottleneck. Inspired by Yan et al. (2020), the probabilities were generated using a readout attention *computed from the messages between edges produced by the GNN from the last Bellman-Ford timestep*. We have found that a single transformer encoder layer followed by a fully-connected layer is sufficient for our task.

**Augmenting Path Capacities** Assuming integer capacities<sup>2</sup> predicting the edge capacities after the augmentation is achieved using *logistic regression* over the possible new *forward* capacities. For each edge  $e_i$  with capacity  $c_{e_i}$ , based on the message generated for this edge by the GNN, we assign probabilities to each number of the range  $[0; c_{e_i}]$ . *Each forward-backward edge capacity pair keeps constant sum.*

To provide unique supervision signal for the above two tasks, random walks of length 5 are generated, together with random integer edge capacities in the range  $[1; 10]$ .

## 4. Evaluation through simulation

Simply evaluating each step separately may not provide sufficient insight on how well the algorithm is learnt – discrepancies in either subroutine can nullify the correctness of the algorithm. Here we present *evaluation through simulation*, which simulates the Ford-Fulkerson from Algorithm 1. Algorithm 2 summarises the simulation. Subroutine details and design decisions are discussed below.

**Finding Augmenting Path and Termination** The main issue with this step is that it is not possible to distinguish whether a valid path does not exist or the network is unable to find it. A trivial heuristic is terminating the algorithm as soon as the network produces an invalid path containing a zero capacity edge. A slightly better approach is a *thresholding heuristic* – pre-defining a threshold hyperparameter  $t$  and terminating the execution if the network is unable to find a path  $t$  consecutive times. To add some non-determinism edge weights are randomised for every attempt.

A smarter approach would be to learn to predict which nodes are reachable in the residual network via edges with positive capacity using the Breadth-First Search (BFS) algorithm. Therefore we can decide to terminate the algorithm, by predicting whether the sink is reachable from the source. If predicted reachable, a possible path from the source to the sink is generated by predicting predecessors. This heuristic

<sup>2</sup>This does not make the problem less general.

### Algorithm 2 Simulated Ford-Fulkerson

---

```

Input:  $G_f, src, sink, oracle$  {Neural network oracle}
 $cnt_b = 1$ 
while  $oracle.FIND-PATH(G_f, src, sink)$  do
     $p = oracle.path$ 
     $c_f(p) = oracle.FIND-PATH(G_f, src, sink, p)$ 
     $real-c_f(p) = \min\{c_f(u, v) : (u, v) \in p\}$ 
     $cnt_b++$ 
    if  $c_f(p) \neq real-c_f(p)$  then
        break
    end if
    if  $real-c_f(p) = 0$  then  $\{t_b$  to avoid endless loops $\}$ 
        if  $cnt_b > t_b$  then
            break
        end if
    end if
     $oracle.SUBTRACT-BOTTLENECK(G_f, src, sink, p, c_f(p))$ 
     $cnt_b = 1$ 
end while
return  $\sum_{v \in G} c_f(v, src)$ 

```

---

is less artificial than the previous one, but now we have no guarantee that the generated path is valid. However, the bottleneck finding subroutine can be used to detect the presence of a zero capacity edge.

**Bottleneck Finding** Similar issue arises here: the network could predict a wrong edge as the bottleneck on the path, making the algorithm incorrect. If such an error occurs, the Ford-Fulkerson algorithm is terminated instantly. Under the bipartite matching setting this can only happen if the generated path is invalid. In such case if the network correctly predicts a zero capacity edge, the path-finding step is rerun again. A similar thresholding logic is applied to avoid endless loops.

**Augmenting Path Capacities** The new predicted capacities are compared against the real ones and if they are different, the Ford-Fulkerson algorithm is terminated. This may appear as a too strict policy, but evaluation on the bipartite matching setting showed that the network learns to accurately perform this step.

**Design Motivation** If any of the above subroutines is wrong the flow value produced will be lower than optimal. Incorrect path-finding will keep generating invalid paths. Badly learnt BFS, bottleneck finding or subtraction can cause premature termination. Additionally, a well-learnt bottleneck finding will allow for reruns to be generated, allowing the network to ‘correct’ itself, to some extent.

The code for neural execution and simulation can be found at <https://anonymous.4open.science/r/da455398-f994-46b9-b707-a05693c63eab/>.

Table 1. Accuracy of finding maximum flow at different graph sizes. Model format is  $\langle$ architecture $\rangle(\langle$ termination-heuristic $\rangle)$ . Termination heuristic is formatted as  $(t = X)$ , where  $X$  is pre-determined. PNA-STD denotes PNA without the std aggregator.

Model	1× scale	2× scale	4× scale	8× scale
MPNN( $t = 1$ )	$97\% \pm 1.61\%$	$90\% \pm 3.46\%$	$97.8\% \pm 2.44\%$	$100\% \pm 0.00\%$
MPNN( $t = 3$ )	$100\% \pm 0.00\%$	$99.4\% \pm 1.28\%$	$100\% \pm 0.00\%$	$100\% \pm 0.00\%$
MPNN( $t = 5$ )	$100\% \pm 0.00\%$	$99.8\% \pm 0.6\%$	$100\% \pm 0.00\%$	$100\% \pm 0.00\%$
MPNN(BFS)	$99.8\% \pm 0.06\%$	$99.8\% \pm 0.06\%$	$100\% \pm 0.00\%$	$100\% \pm 0.00\%$
PNA-STD(BFS)	<b><math>100\% \pm 0.00\%</math></b>	<b><math>100\% \pm 0.00\%</math></b>	<b><math>100\% \pm 0.00\%</math></b>	<b><math>100\% \pm 0.00\%</math></b>

## 5. Evaluation

**Dataset and training details** 300 bipartite graphs are generated for training and 50 for validation. The probability of generating an edge between the two subsets was fixed at  $p = \frac{1}{4}$ . Bipartite graph subset size was fixed at 8 as smaller sizes generated too few training examples. Both subset were chosen to have the same size, as the maximum flow (maximum matching) is dictated from the size of the smaller subset. We learn to execute all subroutines simultaneously. Adam optimiser (Kingma & Ba, 2015) was used for training (initial learning rate 0.0005, batch size 32) and early stopping with patience of 10 epochs on the last step predecessor validation accuracy was performed. Evaluating the ability to strongly generalise is performed on graphs with subset size 8, 16, 32 and 64 (50 graphs each). Standard deviations are obtained over 10 simulation runs.

**Architectural details** Two types of GNNs are assessed for their ability to learn to execute the Ford-Fulkerson algorithm. These are Message-passing neural networks (MPNN) with maximisation aggregation rule (Gilmer et al., 2017) and Principal Neighbourhood Aggregation (PNA) (Corso et al., 2020) with the standard deviation (std) aggregator removed<sup>3</sup>. Latent feature dimension was fixed to  $K = 32$  features. Inputs (capacities and weights) are given as 8-bit binary numbers. (Infinity is represented as the bit vector 111...1.) Similar to Yan et al. (2020), embedding vector  $\vec{v}_i$  is learnt for each bit position. For each  $n$ -bit input  $\vec{x}$ , the input feature embedding is computed as  $\vec{x} = \sum_{i=0}^{n-1} x_i \vec{v}_i$ .

**Results and discussion** All results are reported on the test set graphs. We report the accuracy of predicting a flow (matching) equal to the *maximum* one. Table 1 presents the accuracy at different scale. Under threshold based execution, only the path finding is performed neurally, since all generated paths will have edges with capacity 1.

An exciting observation is that even a threshold of 1, i.e. terminating Ford-Fulkerson as soon as an invalid path is generated yields high accuracy – about 90% for the 2× scale and more than 95% for other datasets. In other words,

<sup>3</sup>The std aggregator for a task with no input noise (such as bipartite matching) results in a model which overfits to the data.

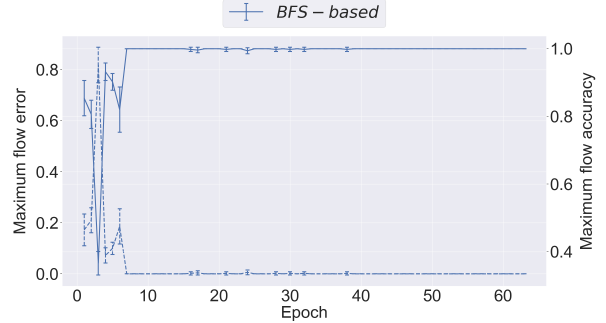


Figure 2. Maximum flow accuracy (solid) and mean absolute flow error (dashed) per epoch for PNA using BFS-based termination.

if a valid path exists, it is likely that the network will find it. A threshold of 3 gives a noticeable boost in the accuracy and a threshold of 5 turns out to be sufficient for a perfect execution (almost 100% accuracy with deviation less than 1%). An MPNN processor, which uses BFS for termination and determines the bottleneck and edge capacities after augmentation performs better than threshold based termination when  $t = 1$  and is comparable to other choices of  $t$ . A further ablation study (Appendix A) showed that the latter two subroutines have infinitesimal impact on the accuracy.

The best performing model is a PNA model using all aggregators but the std one. The accuracy per epoch for the 1× scale is given in Figure 2. The network exhibits some initial instability during the first epochs, but quickly converges to almost 100% accuracy which is retained until the training ends. The best model also yields 100% accuracy at all scales, but our additional experiments (Appendix B) revealed that dropping the std aggregator is critical.

To further evaluate the strong generalisation ability, the two best-performing models were tested on bipartite graphs generated with different edge probability. 50 more test examples were generated for each of  $scale \in \{1\times, 2\times\}$  and  $p \in \{\frac{1}{5}, \frac{1}{2}, \frac{3}{4}\}$ . Both models performed equivalently and exhibited average accuracy higher than 99.73% across all test sets. Further details in Appendix C.

We have for the first time shown (near-)perfect strong generalisation for a complex algorithmic execution task. We hope this paves the way to further related applications.

## References

Bellman, R. On a routing problem. *Quarterly of Applied Mathematics*, 16(1):87–90, 1958. ISSN 0033569X, 15524485. URL <http://www.jstor.org/stable/43634538>.

Boykov, Y. and Funka-Lea, G. Graph cuts and efficient N-D image segmentation. *Int. J. Comput. Vis.*, 70(2):109–131, 2006. doi: 10.1007/s11263-006-7934-5. URL <https://doi.org/10.1007/s11263-006-7934-5>.

Cormen, T. H., Leiserson, C. E., Rivest, R. L., and Stein, C. *Introduction to Algorithms*, 3rd Edition. MIT Press, 2009. ISBN 978-0-262-03384-8. URL <http://mitpress.mit.edu/books/introduction-algorithms>.

Corso, G., Cavalleri, L., Beaini, D., Liò, P., and Veličković, P. Principal neighbourhood aggregation for graph nets. *CoRR*, abs/2004.05718, 2020. URL <https://arxiv.org/abs/2004.05718>.

Ford, L. R. and Fulkerson, D. R. Maximal flow through a network. In *Canadian Journal of Mathematics*, pp. 399–404, 1956.

Gilmer, J., Schoenholz, S. S., Riley, P. F., Vinyals, O., and Dahl, G. E. Neural message passing for quantum chemistry. In *Proceedings of the 34th International Conference on Machine Learning, ICML 2017, Sydney, NSW, Australia, 6-11 August 2017*, pp. 1263–1272, 2017. URL <http://proceedings.mlr.press/v70/gilmer17a.html>.

Hamrick, J. B., Allen, K. R., Bapst, V., Zhu, T., McKee, K. R., Tenenbaum, J., and Battaglia, P. W. Relational inductive bias for physical construction in humans and machines. In *Proceedings of the 40th Annual Meeting of the Cognitive Science Society, CogSci 2018, Madison, WI, USA, July 25-28, 2018*, 2018. URL <https://mindmodeling.org/cogsci2018/papers/0341/index.html>.

Kingma, D. P. and Ba, J. Adam: A method for stochastic optimization. In *3rd International Conference on Learning Representations, ICLR 2015, San Diego, CA, USA, May 7-9, 2015, Conference Track Proceedings*, 2015. URL <http://arxiv.org/abs/1412.6980>.

Veličković, P., Ying, R., Padovano, M., Hadsell, R., and Blundell, C. Neural execution of graph algorithms. In *International Conference on Learning Representations*, 2020. URL <https://openreview.net/forum?id=SkgKO0EtvS>.

Xu, K., Li, J., Zhang, M., Du, S. S., Kawarabayashi, K., and Jegelka, S. What can neural networks reason about? In *8th International Conference on Learning Representations, ICLR 2020, Addis Ababa, Ethiopia, April 26-30, 2020*, 2020. URL <https://openreview.net/forum?id=rJxbJeHFPs>.

Yan, Y., Swersky, K., Koutra, D., Ranganathan, P., and Hashemi, M. Neural execution engines, 2020. URL <https://openreview.net/forum?id=rJg7BA4YDr>.

## A. Subroutine impact

An ablation study of an MPNN based model (Table 2, top half) shows that using the network to perform the bottleneck finding and/or augmentation steps has minimal impact on the overall accuracy: In almost all cases accuracy remains the same (100%) with occasional difference of 0.2% on 1 $\times$  and 2 $\times$  scales. This is further supported by the following two observations. Setting an edge with capacity 0 to be a negative example and edge with 1 – positive, the average true negative rate for finding the bottleneck across all scales is 0.9928. The average augmentation accuracy (correctness of capacities after augmentation) is 0.9995.

## B. Removing STD aggregator is critical

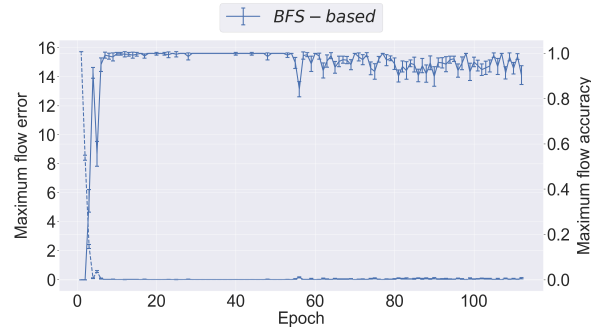


Figure 3. PNA on 2 $\times$  scale. The model shows signs of overfitting.

Our initial experiments with the PNA architecture (Table 2) did not align with our expectations – PNA model which only finds the augmenting path neurally performs significantly worse than MPNN on the 2 $\times$  scale which neurally executes all subroutines. Plotting the accuracy per epoch for that scale reveals that the accuracy worsens for the second half of the training. Our hypothesis was that since the task of finding maximum flow is deterministic and contains no noise, the std aggregator leads to overfitting. This was confirmed by obtaining 100% accuracy (Table 1, bottom, all subroutines performed neurally) across all scales by a model which drops the aggregator.

Table 2. Accuracy of finding maximum flow at graph sizes. Model format is as in Table 1. *-bottle* (minus bottleneck) corresponds to changing the neural execution of bottleneck finding to a deterministic one. *-augment* is used when the augmentation step is deterministic.

Model	Accuracy			
	1× scale	2× scale	4× scale	8× scale
MPNN(BFS)	99.8% ± 0.06%	99.8% ± 0.06%	100% ± 0.00%	100% ± 0.00%
MPNN(BFS) <i>-bottle</i>	100% ± 0.00%	99.8% ± 0.06%	100% ± 0.00%	100% ± 0.00%
MPNN(BFS) <i>-augment</i>	100% ± 0.00%	100% ± 0.00%	100% ± 0.00%	100% ± 0.00%
MPNN(BFS) <i>-augment</i> <i>-bottle</i>	100% ± 0.00%	100% ± 0.00%	100% ± 0.00%	100% ± 0.00%
PNA(BFS)	100% ± 0.00%	92.8% ± 2.56%	99.8% ± 0.6%	100% ± 0.00%
PNA(BFS) <i>-bottle</i>	100% ± 0.00%	92.8% ± 2.56%	99% ± 1.34%	100% ± 0.00%
PNA(BFS) <i>-augment</i>	100% ± 0.00%	93% ± 4.31%	99% ± 0.10%	100% ± 0.00%
PNA(BFS) <i>-augment</i> <i>-bottle</i>	100% ± 0.00%	94.0% ± 2.68%	99.6% ± 0.8%	100% ± 0.00%

Table 3. Accuracy at different edge probability  $p$  for the two best models.

Scale	Model	Accuracy		
		$p = \frac{1}{5}$	$p = \frac{1}{2}$	$p = \frac{3}{4}$
1×	MPNN(BFS)	100% ± 0.00%	100% ± 0.00%	100% ± 0.00%
	PNA-STD(BFS)	100% ± 0.00%	100% ± 0.00%	100% ± 0.00%
2×	MPNN(BFS)	99.2% ± 0.98%	100% ± 0.00%	100% ± 0.00%
	PNA-STD(BFS)	99.4% ± 0.92%	100% ± 0.00%	100% ± 0.00%

## C. Varying edge probability

Table 3 shows the accuracy for two best models on data generated with different edge probability  $p$ . Higher  $p$  produces cases easily solved by both models. The accuracy is slightly less (99%) only for lower edge probability at 2× scale. Both processor architectures perform equivalently.